Hydrothermal Synthesis of Zn_2SnO_4 Nanoparticles for Ethanol Sensor

Lai Van Duy, Nguyen Hong Hanh, Nguyen Duc Hoa[+], Chu Manh Hung[*]
Hanoi University of Science and Technology – No. 1, Dai Co Viet Str., Hai Ba Trung, Ha Noi, Viet Nam
Received: April 05, 2019; Accepted: June 24, 2019

Abstract

Zn_2SnO_4 nanoparticles were synthesized by a facile hydrothermal method for a C_2H_5OH gas-sensing application. The synthesized materials were characterized by field-emission scanning electron microscopy, powder x-ray diffraction and Raman spectroscopy. Gas sensing characteristics were measured at various concentrations of C_2H_5OH in temperature ranging from 350 to 450°C. Results pointed out that the sensor showed the highest response values at operating temperature of 450°C. The sensor response increased linearly with ethanol concentrations in the range of 125–1500 ppm. The results indicated that the hydrothermally synthesized Zn_2SnO_4 nanoparticles might be a promising candidate material for C_2H_5OH gas sensor.

Keywords: Hydrothermal, SEM, Characteristics; gas sensor

1. Introduction

Ethanol is one of the most important individual organic compounds which has been readily available all over the world. This compound is widely used as an intermediate for the synthesis of other organic compounds such as acetaldehyde, glycol, ethylamine, ethyl acetate, acetic acid, ethyl chloride, and so on [1]. However, long-term exposure to ethanol can cause central nervous system disorders. Therefore, detection and monitoring of ethanol gas timely become a very important issue regarding to the production safety. In addition, ethanol sensors can be used in various fields including of clinical diagnosis [2].

Resistive type gas sensors commonly use binary oxides as sensing materials such as ZnO, TiO_2, SnO_2, In_2O_3, Fe_2O_3, WO_3, CuO and NiO [3]. However, they suffer from some limitations such as low sensitivity, poor selectivity and instability. In recent years, the complex oxides are of great interest as gas sensitive materials because they have many advantages over the common binary oxides such as chemically inert, thermal stable, as well as environmentally friendly. The complex oxides extensively used as sensor materials are $ZnFe_2O_4$ [4], [5], and Zn_2SnO_4 [6], [7] because of their multi-functional characteristics including of high electron mobility, high electrical conductivity. Among other, Zn_2SnO_4 (ZTO) is an important n-type transparent semiconductor with a band gap of 3.6 eV [6]. There are numerous researches on Zn_2SnO_4 synthesized by hydrothermal [8], [9], co-precipitation [10], sol-gel [11], electrospinning [4], [5], thermal evaporation [6], [7]and so on. Due to its good thermal stability, high chemical sensitivity, and low-visibility absorption. ZTO has been widely studied in the fields of gas sensor [6], [12]. By utilizing hydrothermal method, researchers could create a huge number of shapes and structures of this material to apply in different fields. However, there is few researches focusing on ethanol gas-sensing applications despite when applied as gas-sensing materials, ZTO can exhibit relatively good sensing properties to some gases [6], [9], [13]–[15].

In this study, we develop a simple hydrothermal method for synthesizing ZTO nanoparticles for effective ethanol gas sensor towards industry application.

2. Experimental

All the reagents were analytical reagent and used without further purification. Zn_2SnO_4 nanoparticles were synthesized by a facile hydrothermal method without any post-thermal calcination. Processes for the synthesis of Zn_2SnO_4 nanoparticles are summarized in Fig.1. In a typical synthesis, $ZnSO_4.7H_2O$ (8 mmol) and $SnCl_4$.$5H_2O$ (4 mmol) were dissolved in 30 mL deionized water. After stirring for 15 min, 20 ml NaOH (32 mmol) solution was added with further stirring for 15 min to adjust the pH value of 8. Then, the above turbid solution was transferred into a 100 mL Teflon-lined stainless-steel autoclave for hydrothermal. The hydrothermal process was maintained at 180°C for 24h. After natural cooling to room temperature, the precipitate was centrifuged and washed with deionized water for several times. The last two times

[*+] Corresponding author: Tel.: (+84) 984050213
Email: hung.chumanh@hust.edu.vn

were washed with ethanol solution and collected by centrifugation at 4000 rpm. Finally, the white product was obtained and dried in an oven at 60ºC for 24 h. The synthesized materials were characterized by powder x-ray diffraction (XRD; Advance D8, Bruker), field-emission scanning electron microscopy (SEM, JEOL 7600F) and Raman spectroscopy was measured using the Renishaw Invia Confocal micro-Raman System.

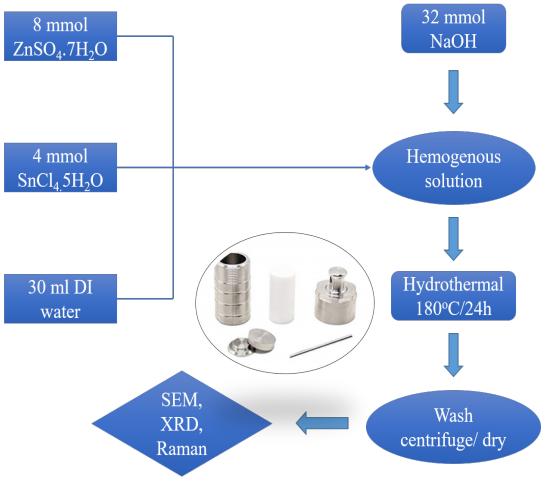

Fig. 1. Process for the hydrothermal synthesis of Zn_2SnO_4 nanoparticles.

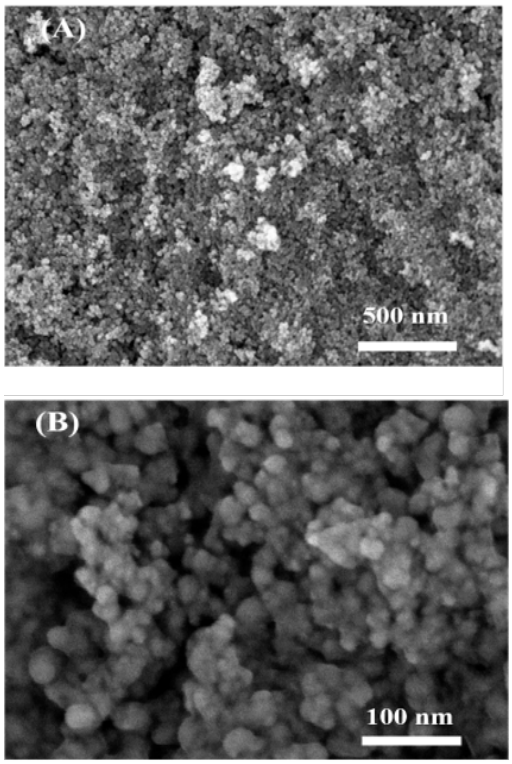

Fig. 2. SEM images of synthesized Zn_2SnO_4 nanoparticles.

3. Results and discussion

Morphology and microstructure of the obtained products were investigated by SEM, and the data are shown in Fig.2. Obviously, the low-magnification SEM image (Fig.2A) demonstrated that the as-prepared products were composed of homogeneous nanoparticles. The high- magnification SEM image (Fig.2B) reveals clearly that the synthesized nanoparticles are in fact agglomerated of much smaller particles. The nanoparticles have a spherical morphology with an average particle size of about 15 nm. It was reported that the smaller nanoparticle size could provide larger adsorption sites for gaseous molecules to adsorb and enhance the gas sensing performances. Herein, the homogenous nanoparticles were obtained without using any surfactant, thus reducing the usage of chemical.

Crystal structure of the synthesized nanoparticles was studied by XRD. As shown in Figure 3(A), the XRD pattern of the synthesized Zn_2SnO_4 nanoparticles indicates that the material has a monoclinic crystal structure (space group Fd3m) with lattice parameters of a = b = c = 0.854 nm. The main diffraction peaks were indexed to (220), (311), (400), (511) and (440) lattice planes of Zn_2SnO_4. The XRD diffraction peaks were well agreed with cubic spinel-structure of Zn_2SnO_4 according to JCPDS Card no.74-2184. No diffraction peak from other impurities can be detected in the XRD pattern. This mean that the synthesized material is pure phase of Zn_2SnO_4 with the accuracy of XRD. The average crystal size of the Zn_2SnO_4 nanoparticles calculated using the Scherer equation was approximately 14.16 nm (Fig.3A). This value is comparable with that of the nanoparticles estimated from the SEM images, indicating the highly crystallinity of the material [7].

The Raman spectrum of the synthesized Zn_2SnO_4 nanoparticles is shown in Fig.3B. It is clearly that three sharp peaks at 678 cm^{-1}, 535 cm^{-1} and 443 cm^{-1} were observed. All three peaks respectively correspond to active vibration modes A_{1g}, E_{2g}, and E_g of Zn_2SnO_4 [16]. It was reported that the mode with the highest intensity at about 678 cm^{-1} is due to the symmetric stretching of the Zn–O bonds in the ZnO_4 tetrahedra of the fully inverse Zn_2SnO_4 spinel. The peak at about 535 cm^{-1} was associated with internal vibrations of the oxygen tetrahedron [17].

The transient resistance versus time upon exposure to different concentrations of C_2H_5OH measured at temperatures ranging from 350°C to 450ºC is shown in Fig.4A. The base resistances of the sensor in air were 22.63 MΩ, 12.65 MΩ, and 3.03 MΩ for temperatures of 350°C, 400°C, and 450°C,

respectively. The resistance of the Zn_2SnO_4 nanoparticles decreases with increasing temperature and exhibits an obvious negative temperature coefficient of resistance in the measured range. The sensor also shows good recovery characteristics where the resistances returned to the initial values when the flow of analytic gas was stopped. Figure 4A also reveals that the response and recovery speeds were improved with increase of working temperature. At all measured temperatures, the sensor shows reversible response characteristics. Reversible adsorption of analytic gas molecules on the surface of the sensing material is very important in the practical application and reusability of gas sensors

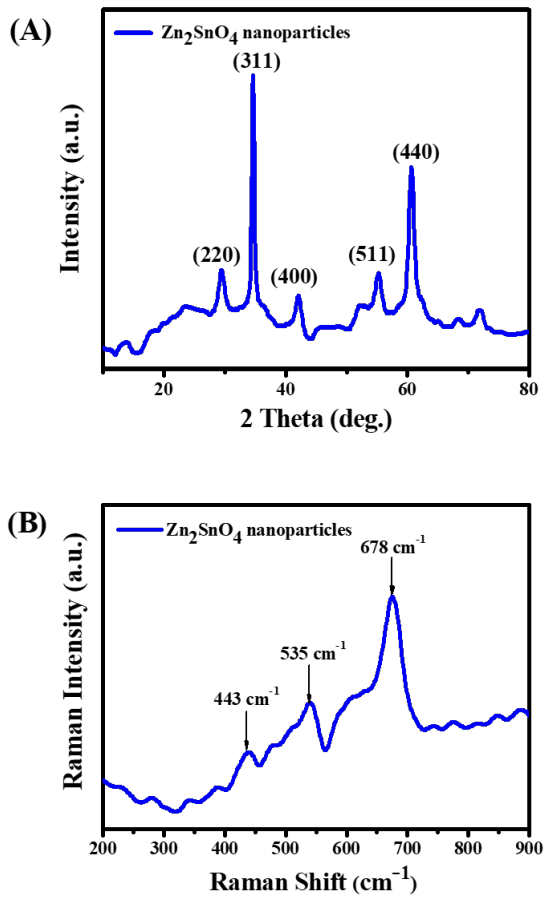

Fig. 3. (A) XRD pattern, (B) and Raman spectrum of the synthesized Zn_2SnO_4 nanoparticles.

The sensor response S (R_a/R_g), as a function of C_2H_5OH concentrations measured at different temperatures, is shown in Fig.4B. At all measured temperatures, the sensor response increases with C_2H_5OH concentrations in the measured range. At a given concentration, the sensor response increases with increasing working temperatures. The response value increases from 2.5 to 6.7 when the C_2H_5OH concentration increases from 125 ppm to 1500 ppm at a measured temperature of 400°C. At 450°C, the response value increases from 4.5 to 16 when the C_2H_5OH concentration increases from 125 ppm to 1500 ppm. The sensor response can be improved by increasing the working temperature to over 450°C. However, increasing the working temperature requires higher energy, but this can lead to damage of microheater. For practical application, the power consumption of the device should be limited; thus, the sensor response at temperatures higher than 450°C were not necessary to characterize.

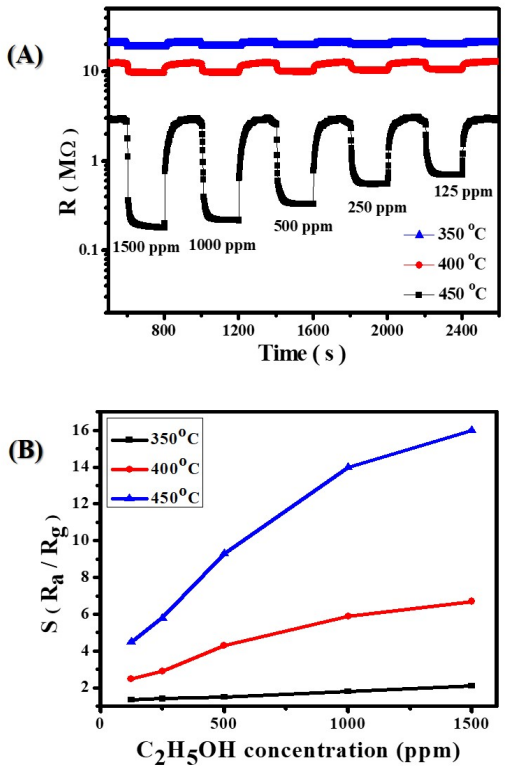

Fig. 4. C_2H_5OH sensing characteristics of Zn_2SnO_4 nanoparticles measured at different temperatures: (A) transient resistance versus time upon exposure to different C_2H_5OH concentrations, (B) gas response as a function of C_2H_5OH concentrations.

The response and recovery times of the sensor when measured at different concentrations of C_2H_5OH at 450ºC working temperature are shown in Fig.5. The response time decreased from 16 s to approximately 4 s when the concentration increased from 125 ppm to 1500 ppm. In reversely, the recovery time increased from 48 s to 79 s when the C_2H_5OH concentration increased from 125 ppm to 1500 ppm. Anyhow, the fast response time of the sensor is very effective for the practical application.

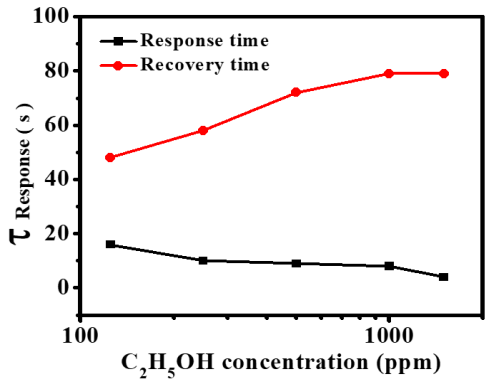

Fig. 5. Response time and recovery times at working temperature 450ºC as functions of C_2H_5OH concentrations

The gas sensing mechanism of metal oxide is based on the adsorption and desorption of gas molecules and chemical reactions on the surface of sensing materials [18]. Zn_2SnO_4 is a well-known n-type conductor. When the sensor is exposed in ambient air, oxygen molecules will adsorb on the surface of Zn_2SnO_4 nanoparticles and ionize to negatively charged surface-adsorbed oxygen species by capturing free electrons from the conducting band of Zn_2SnO_4 nanoparticles, as shown in Eqs. (1) - (3):

$$O_2\,(gas) \rightarrow O_2\,(ads) \quad (1)$$

$$O_2\,(ads) + e^- \rightarrow O^{2-}\,(ads) \quad (2)$$

$$O^{2-}\,(ads) + e^- \rightarrow 2O^-\,(ads) \quad (3)$$

As a result, a thick electron depletion layer will form on the surface of Zn_2SnO_4 nanoparticles, and a high potential barrier is formed between the adjacent nanograins. When the sensor is exposed to reducing gas such as ethanol at a moderate temperature, the ethanol molecules would react with the surface adsorbed oxygen species and the captured electrons are released back to the conduction band, resulting in a deceasing resistance of the sensor. The reaction process between surface adsorbed oxygen species and ethanol is described as Eqs. (4)-(6):

$$C_2H_5OH + 36O_2^- \rightarrow 2CO_2 + 3H_2O + 3e^- \quad (4)$$

$$C_2H_5OH + 6O^- \rightarrow 2CO_2 + 3H_2O + 6e^- \quad (5)$$

$$C_2H_5OH + 6O^{2-} \rightarrow 2CO_2 + 3H_2O + 12e^- \quad (6)$$

A combative result of the fabricated sensor with other reports is summarized in Table 1. The ZnO nanowires processed the highest response, followed by the ZnO nanoplates, SnO_2 hollow sphere, and **α-**Fe_2O_3 nanoparticles. The high working temperature and low sensitivity of bare NPs-based current sensor limit its potential application. Therefore, the controlled synthesis of highly sensitive ethanol sensor that operate at low temperature is mandatory for future sensor applications.

Table 1. Comparative C_2H_5OH gas response of different metal oxide sensors.

Metal oxide sensors	Temp. (ºC)	Gas conc. (ppm)	S (R_a/R_g)	Ref.
α-Fe_2O_3 nanoparticles	200	200	1.3	[19]
ZnO nanoplate	450	100	4	[20]
SnO_2 hollow sphere	450	100	5	[21]
ZnO nanowire	350	500	3.88	[22]
ZnO nanowire	325	50	7	[23]
Zn_2SnO_4 nanoparticles	450	1500	16	This work

4. Conclusion

We introduced a facile and scalable hydrothermal synthesis of Zn_2SnO_4 nanoparticles for effective C_2H_5OH gas-sensing applications. The obtained particles performed a good crystallinity and dispersing level. The mean grain size of Zn_2SnO_4 nanoparticles is about 14.16 nm. The obtained Zn_2SnO_4 nanoparticles exhibit excellent gas sensing properties to ethanol, in terms of high response, fast response and recovery times. The results show that Zn_2SnO_4 nanoparticles can be a potential candidate for high performance ethanol gas sensing material.

Acknowledgment

This research is funded by Hanoi University of Science and Technology (HUST) under the project number T2018-PC-076.

References

[1] L. Meng; Elsevier Inc, Chapter 11 - Ethanol in Automotive Applications, (2019) 289-303.

[2] N. Kien, C. M. Hung, T. M. Ngoc, D. Thi, T. Le, and N.D. Hoa; Low-temperature prototype hydrogen sensors using Pd-decorated SnO_2 nanowires for exhaled breath applications; Sensors Actuators B. Chem. 253 (2017) 156–163.

[3] C. M. Hung, D. Thi, T. Le, and N. Van Hieu; On-chip growth of semiconductor metal oxide nanowires for gas sensors: A review; J. Sci. Adv. Mater. Devices. 2 (2017) 263-285..

[4] N. Van Hoang, C. M. Hung, N. D. Hoa, N. Van Duy, and I. Park; Chemical Excellent detection of H_2S gas at ppb concentrations using $ZnFe_2O_4$ nanofibers loaded with reduced graphene oxide; Sensors Actuators B. Chem. 282 (2018) 876–884.

[5] N. Van Hoang, C. M. Hung, N. D. Hoa, N. Van Duy, and N. Van Hieu; Facile on-chip electrospinning of $ZnFe_2O_4$ nanofiber sensors with excellent sensing performance to H_2S down ppb level; J. Hazard. Mater. 360 (2018) 6-16.

[6] H. X. Thanh, D. D. Trung, K. Q. Trung, K. V. Dam, N. Van Duy, C.M. Hung, N.D. Hoa, N. Van Hieu; On-chip growth of single phase Zn_2SnO_4 nanowires by thermal evaporation method for gas sensor application; J. Alloys Compd. 708 (2017) 470-475.

[7] C. M. Hung, H.V. Phuong, N. Van Duy, N.D. Hoa, and N. Van Hieu; Comparative effects of synthesis parameters on the NO_2 gas-sensing performance of on-chip grown ZnO and Zn_2SnO_4 nanowire sensors; J. Alloys Compd. 765 (2018) 1237-1242.

[8] A. X. Yang, H. Gao, and L. Zhao, Enhanced gas sensing properties of monodisperse Zn_2SnO_4 octahedron functionalized by PdO nanoparticals, Sensors Actuators B. Chem. 266 (2018) 302-310.

[9] H. M. Yang, S.Y. Ma, H.Y. Jiao, Q. Chen, Y. Lu, W.X. Jin, W.Q. Li, T.T. Wang, X.H. Jiang, Z. Qiang, H. Chen, Synthesis of Zn_2SnO_4 hollow spheres by a template route for high-performance acetone gas sensor; Sensors Actuators B. Chem. 245 (2017) 493–506.

[10] X. Lian and Y. Li; Synthesis of Zn_2SnO_4 via a co-precipitation method and its gas-sensing property toward ethanol; Sensors Actuators B. Chem. 213 (2015) 155-163.

[11] K. A. Bhabu, J. Theerthagiri, J. Madhavan, and T. Balu; Synthesis and characterization of zinc stannate nanomaterials by sol- gel method; Materials Science Forum. 832 (2015) 144–157.

[12] J. Yang, S. Wang, L. Zhang, R. Dong, Z. Zhu, and X. Gao; Zn_2SnO_4-doped SnO_2 hollow spheres for phenylamine gas sensor application; Sensors Actuators B. Chem. 239 (2017) 857-864.

[13] T. Xu, X. Zhang, Z. Deng, L. Huo, and S. Gao; Synthesis of Zn_2SnO_4 octahedron with enhanced H_2S gas-sensing performance; Polyhedron. 151 (2018) 510–514.

[14] S. Zn, W. X. Jin, X. H. Jiang, and T. T. Wang Wang, Self-assembly of Zn_2SnO_4 hollow micrtocubes and enhanced gas-sensing performances; Materials Letters. 182 (2016) 264-268.

[15] Q. Zhao, D. Ju, X. Song, X. Deng, M. Ding, and X. Xu; Polyhedral Zn_2SnO_4: Synthesis, enhanced gas sensing and photocatalytic performance; Sensors Actuators B. Chem. 229 (2016) 627–634.

[16] V. Sepel, S.M. Becker, I. Bergmann, S. Indris, M. Scheuermann, M. Bruns, N. St; Nonequilibrium structure of Zn_2SnO_4 spinel nanoparticles; J. Mater. Chem. 22 (2012) 3117.

[17] Q. Zhao, X. Deng, M. Ding, J. Huang, D. Ju, and X. Xu; Synthesis of hollow cubic Zn_2SnO_4 sub-microstructures with enhanced photocatalytic performance; J. Alloys Compd. 671 (2016) 328-333.

[18] D. An, N. Mao, G. Deng, Y. Zou, Y. Li, T. Wei, X. Lian; Ethanol gas-sensing characteristic of the Zn_2SnO_4 nanospheres; Ceram. Int. 42 (2016) 3535–3541.

[19] D. K. Bandgar, S. T. Navale, G. D. Khuspe, S. A. Pawar, R. N. Mulik, and V. B. Patil; Novel route for fabrication of nanostructured α-Fe_2O_3 gas sensor; Mater. Sci. Semicond. Process. 17 (2014) 67–73.

[20] C. Wang, L. Yin, L. Zhang, D. Xiang, and R. Gao; Metal Oxide Gas Sensors: Sensitivity and Influencing Factors; Sensors. 10 (2010) 2088–2106.

[21] B. Wang, L. Sun, and Y. Wang; Template-free synthesis of nanosheets-assembled SnO_2 hollow spheres for enhanced ethanol gas sensing; Mater. Lett. 218 (2018) 290–294.

[22] Y. Wu, T. Jiang, T. Shi, B. Sun, Z. Tang, and G. Liao; Au modified ZnO nanowires for ethanol gas sensing; Sci. China Technol. Sci. 60 (2017) 71–77.

[23] N. S. Ramgir et al.; Ethanol sensing properties of pure and Au modified ZnO nanowires; Sensors Actuators B Chem. 187 (2013) 313–318.